

Polymeric Mach-Zehnder interferometer using serially coupled microring resonators

George T. Paloczi, Yanyi Huang, and Amnon Yariv

Department of Applied Physics, California Institute of Technology, Pasadena, CA 91125 USA
paloczi@caltech.edu, ayariv@caltech.edu

Shayan Mookherjea

Department of Computer and Electrical Engineering, University of California, San Diego, La Jolla, CA 92093 USA

Abstract: We propose a novel geometry for a Mach-Zehnder interferometer in which one arm of the interferometer consists of serially coupled microresonators and the other a simple ridge waveguide. The device was fabricated in an optical polymer and its spectral characteristics were measured at telecommunications wavelengths. The serially coupled rings are modeled using a simple transfer matrix approach. Good agreement is found between the measurement and the theory.

©2003 Optical Society of America

OCIS codes: (130.0130) Integrated Optics, (130.2790) Guided Waves, (230.5750) Resonators, (160.5470) Polymers

References and links

1. K. Oda, N. Takato, and H. Toba, "A wide-FSR double-ring resonator for optical FDM transmission systems," *IEEE J. Lightwave Tech.* **9**, 728-736 (1991).
2. R. Orta, P. Savi, R. Tascone, and D. Trinchero, "Synthesis of multiple-ring-resonator filters for optical systems," *IEEE Phot. Tech. Lett.* **7**, 1447-1449 (1995).
3. B. E. Little, S. T. Chu, H. A. Haus, J. Foresi, and J. -P. Laine, "Microring resonator channel dropping filter," *IEEE J. Lightwave Tech.* **15**, 998-1005 (1997).
4. J. V. Hryniewicz, P. P. Absil, B. E. Little, R. A. Wilson, and P. -T. Ho, "Higher order filter response in coupled microring resonators," *IEEE Phot. Tech. Lett.* **12**, 320-322 (2000).
5. A. Melloni, and M. Martinelli, "Synthesis of direct-coupled-resonators bandpass filters for WDM systems," *IEEE J. Lightwave Tech.* **20**, 296-303 (2002).
6. A. Yariv, Y. Xu, R. K. Lee, and A. Scherer, "Coupled resonator optical waveguide: a proposal and analysis," *Optics Lett.* **24**, 711-713 (1997).
7. Y. Xu, R. K. Lee, and A. Yariv, "Propagation and second harmonic generation of electromagnetic waves in a coupled-resonator optical waveguide," *J. Opt. Soc. Am. B* **17**, 387-400 (2000).
8. S. Mookherjea, and A. Yariv, "Kerr-stabilized super-resonant modes in coupled-resonator optical waveguides," *Phys. Rev. E* **66**, 046610 (2002).
9. J. K. S. Poon, S. Mookherjea, G. T. Paloczi, Y. Huang, and A. Yariv, "Matrix analysis of microring coupled-resonator optical waveguides," (submitted).
10. A. Martinez, A. Griol, P. Sanchis, and J. Marti, "Mach-Zehnder interferometer employing coupled-resonator optical waveguides," *Opt. Lett.* **28**, 405-407 (2003).
11. M. Bayindir, B. Temelkuran, and E. Ozbay, "Tight-binding description of the coupled defect modes in three dimensional photonic crystals," *Phys. Rev. Lett.* **84**, 2140-2143 (2000).
12. K. Kawano, and T. Kitoh, *Introduction to optical waveguide analysis* (Wiley, 2001), Chap. 4.
13. A. Yariv, "Universal relations for coupling of optical power between microresonators and dielectric waveguides," *Electronics Lett.* **36**, 321-322 (2000).

1. Introduction

Serially coupled microresonators have been studied as optical filters exhibiting large free spectral range [1] or higher-order filter characteristics [2-5]. In addition, it was recently shown

that serially coupled microresonators present a fundamentally new form of waveguiding different from that which is based on total internal reflection or Bragg guidance. This new class of waveguides has been termed coupled-resonator optical waveguides (CROWs) [6]. For the case of an infinite number of resonators, each weakly coupled only to nearest-neighboring resonators, a simple tight-binding formalism can accurately analyze the CROW. In this limit, CROWs can exhibit reduced group velocity dependent only on nearest neighbor mode overlap integrals. The reduction in group velocity can improve the efficiency of nonlinear frequency conversion and, in the limit of zero group velocity, result in “frozen” pulses [7,8]. For the present analysis we employ an alternative analysis method in which each coupling section is represented by a coupling matrix and the phase and loss accumulated in the resonator are represented by a propagation matrix. By cascading the matrices, the transmission of the CROW is built up for an arbitrary series of resonators with arbitrary coupling between them. The model used here embodies a more general approach restricted to neither the special case of weak coupling, nor an infinite number of resonators. The convergence of the matrix and tight-binding methods and an investigation on the limits of validity of the tight-binding method will be presented elsewhere [9].

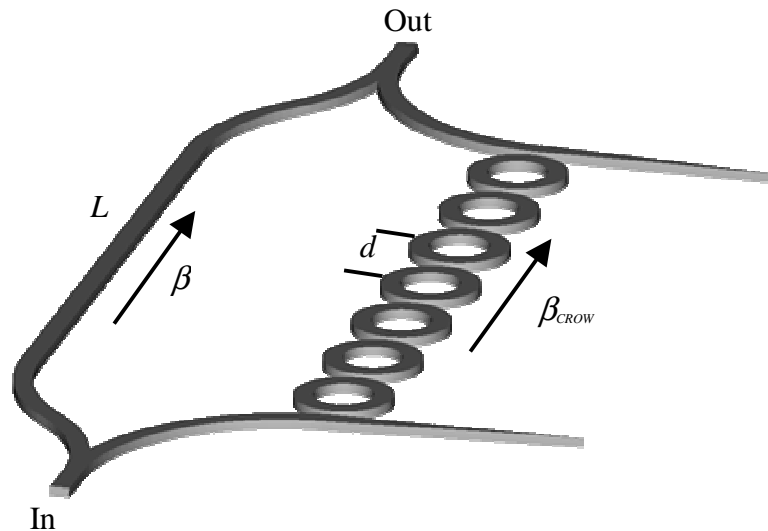


Fig. 1. Schematic diagram of a CROW-MZI with one arm as a ridge waveguide of length L , with propagation constant β and the other arm consisting of coupled microresonators, spaced by a distance d , with propagation constant β_{CROW} . Y-branches divide and add the optical field equally between the two arms. Adiabatic tapers act as impedance matched terminations after the field couples to the first resonator, ensuring no back reflected fields.

The Mach-Zehnder interferometer (MZI) presents one of the simplest geometries for interrogating optical phase characteristics of waveguides through interference. A MZI composed completely of coupled photonic crystal defects was proposed and fabricated with aluminum rods, and interference nulls were observed in the microwave regime [10]. However, by incorporating a CROW as only one path of the MZI, interference occurs between the field amplitudes of a waveguide whose phase properties we know (conventional ridge waveguide) and a waveguide whose phase properties we are interested in (CROW). A similar concept was used to investigate light propagation for coupled defects in an aluminum rod photonic crystal by measuring the interference of microwaves in free-space and in the coupled-defect device [11]. A schematic diagram of the CROW-MZI device we propose is illustrated in Fig. 1. In

this report, we demonstrate a CROW-MZI fabricated in a polymeric waveguide material for operation near telecommunications wavelengths ($\lambda \approx 1550$ nm). Good agreement is found between the measured results and the predictions of the matrix theory.

2. Fabrication and measurement

The devices were prepared by first spinning a $1.6\ \mu\text{m}$ thick optical core layer of a negative novalac epoxy SU-8 ($n=1.565$, available from Micro-Chem Corp.) onto a silicon wafer with $5\ \mu\text{m}$ of thermal silicon-oxide serving as the lower cladding. Waveguides of width $2\ \mu\text{m}$ were directly patterned by electron beam crosslinking of the SU-8 core using a scanning electron microscope (SEM). The end facets of the waveguides were left as prepared by cleaving the substrate. The racetrack resonators had semi-circular sections of radius $100\ \mu\text{m}$, and $50\ \mu\text{m}$ long parallel coupling regions. The waveguides in the coupling section were separated by $750\ \text{nm}$, although further SEM investigation revealed a layer of residual SU-8 between the waveguides, decreasing the effective separation and increasing the coupling beyond what would be expected for a $750\ \text{nm}$ gap. The effective refractive index of the waveguide was calculated to be 1.485 by semi-vectorial finite difference simulation [12]. The free spectral range of an individual resonator is therefore $2.2\ \text{nm}$ for transverse electric (TE) polarized light in the vicinity of the $1550\ \text{nm}$ telecommunication band. An optical microscope image of the entire device is shown in Fig. 3(a). In Fig. 3(b), we show an angle-view SEM image of two waveguides converging into a coupling section, and in Fig. 3(c), a close-up top-view SEM image of the coupling region.

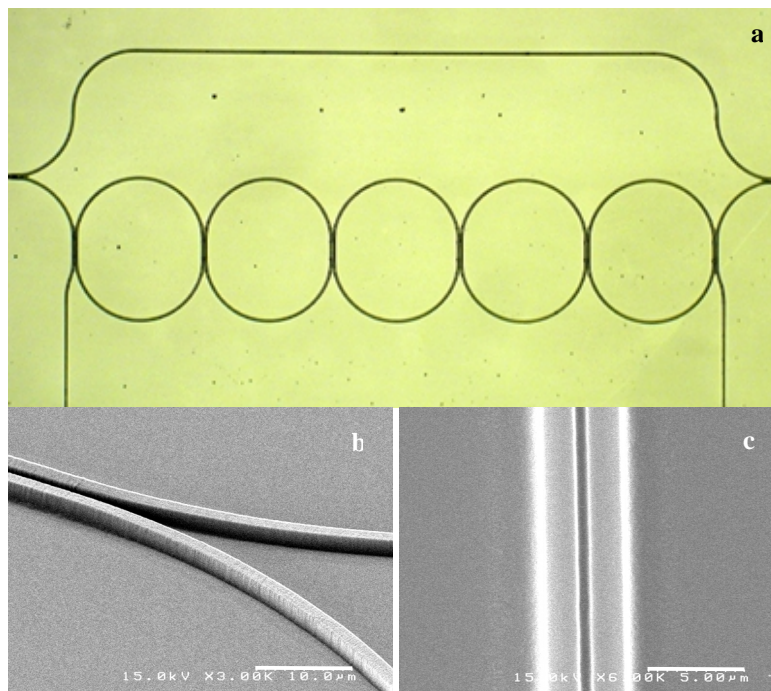


Fig. 2. (a) Optical microscope image of the CROW-MZI showing a total device width of approximately $1.2\ \text{mm}$. The identical racetrack microresonators had $50\ \mu\text{m}$ straight coupling sections and $100\ \mu\text{m}$ bend radii in the curved sections. (b) Angle-view SEM image of two waveguides converging into the coupling section, showing straight side-walls and indicating overall waveguide smoothness. (c) Top-view SEM image of coupling section showing $2\ \mu\text{m}$ wide waveguides separated by $750\ \text{nm}$.

For measurement, a tunable laser diode provided the input TE-polarized optical signal via a polarization controller and a tapered single-mode fiber. The device output was collected by a

20x microscope objective focused on either an infrared CCD for viewing or a photodetector for measurement. Both the tunable laser and the photodetector measurement were controlled by computer. Shown in Fig. 3 is a measured spectrum of the CROW-MZI transmission for an input wavelength scan of 50 nanometers, ranging from 1500 to 1550 nanometers, covering approximately 22 individual-resonator free spectral ranges. The output spectrum shows an intricate, but essentially periodic, interferometric waveform.

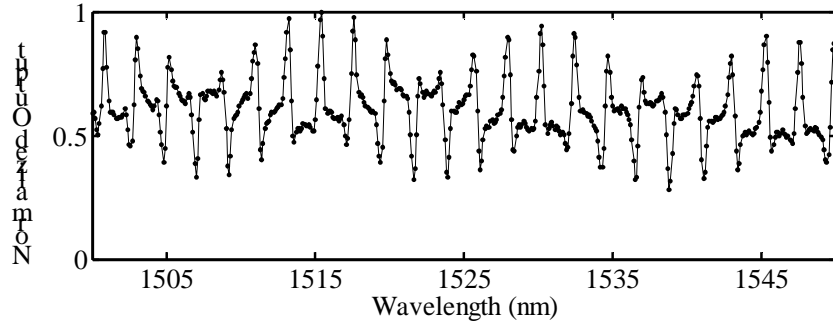


Fig. 3. Normalized measured output power of the polymer CROW-MZI ranging over a spectral bandwidth of 50 nanometers, approximately 22 single resonator free spectral ranges.

3. Comparison to theory

We describe the optical response of a CROW with a unidirectional (2 x 2) matrix model incorporating the evanescent ring-to-ring coupling and the propagation within each ring [2,9,13]. The notation for the complex field amplitudes of the CROW device is shown in Fig. 4.

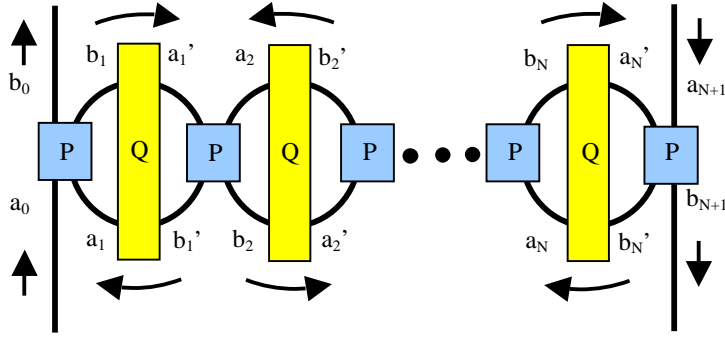


Fig. 4. Coupled resonator optical waveguide with N rings (N odd for the output direction as shown). The arrows signify the direction of light propagation. The matrix P represents the coupling segments and Q accounts for the phase and loss accumulated in the resonators.

The (assumed lossless) evanescent coupling of two waveguides is given by the well-known coupling matrix of coupled-mode theory [13]

$$\begin{pmatrix} b'_n \\ b_{n+1} \end{pmatrix} = \begin{pmatrix} t & \kappa \\ -\kappa^* & t^* \end{pmatrix} \begin{pmatrix} a'_n \\ a_{n+1} \end{pmatrix}, \quad |t|^2 + |\kappa|^2 = 1 \quad (1)$$

where κ denotes the normalized coupling and t the transmitted field past the coupler. These are determined by the physical separation between the two coupled waveguides. Relation (1) can be rewritten in the form

$$\begin{pmatrix} a_{n+1} \\ b_{n+1} \end{pmatrix} = \mathbf{P} \begin{pmatrix} a'_n \\ b'_n \end{pmatrix}, \quad \mathbf{P} = \frac{1}{\kappa} \begin{pmatrix} -t & 1 \\ -1 & t^* \end{pmatrix}. \quad (2)$$

The optical phase and the waveguide loss accumulated over a half-ring distance is given by a propagation matrix

$$\begin{pmatrix} a'_n \\ b'_n \end{pmatrix} = \mathbf{Q} \begin{pmatrix} a_n \\ b_n \end{pmatrix}, \quad \mathbf{Q} = \begin{pmatrix} 0 & e^{-i\beta\pi R - \alpha\pi R} \\ e^{i\beta\pi R + \alpha\pi R} & 0 \end{pmatrix} \quad (3)$$

where α is the absorption coefficient per unit length, R is the ring radius, and $\beta = 2\pi n_{\text{eff}} / \lambda_0$ is the propagation constant of the waveguide. For the case of N -I resonators with N coupling regions, we form the full transmission matrix of the CROW by cascading the matrices \mathbf{P} and \mathbf{Q} :

$$\begin{pmatrix} a_{N+1} \\ b_{N+1} \end{pmatrix} = (\mathbf{PQ})_N (\mathbf{PQ})_{N-1} (\dots) (\mathbf{PQ})_2 \mathbf{P}_1 \begin{pmatrix} a_0 \\ b_0 \end{pmatrix} = \mathbf{T} \begin{pmatrix} a_0 \\ b_0 \end{pmatrix}. \quad (4)$$

For simplicity we adopt the notation

$$\mathbf{T} = \begin{pmatrix} A & B \\ C & D \end{pmatrix}. \quad (5)$$

Assuming an input a_0 , taking $a_{N+1}=0$, the output complex field amplitudes normalized to the input are

$$\frac{b_0}{a_0} = -\frac{A}{B}, \quad \frac{b_{N+1}}{a_0} = C - \frac{AD}{B}. \quad (6)$$

In resonant optical systems, small parameter deviations due to slight fabrication errors typically result in unintended spectral features. For instance, small deviations (fractions of a wavelength) in the radii of the N -I constituent resonators result in different resonance frequencies that potentially spoil sharp spectral transmission features of a CROW device. Furthermore, the transmission is very sensitive to small differences (tens of nm) in the N gaps between the coupled waveguides that comprise the CROW. Thus for a proper analysis of the device fabricated and measured here, we would expect the need for N -I fitting parameters for the ring radii and N for the coupling sections. In addition, other variables to be included in the fit are: the length of the ridge waveguide arm, the waveguide loss per unit length, the polarization mixing ratio, the waveguide effective refractive index for both polarizations, and the overall wavelength shift.

To greatly simplify the analysis, we undertake the assumption of single values for the resonator radii and coupling coefficients. Considering this special case of Eq. 4 with identical matrices \mathbf{P} and \mathbf{Q} , the transmission matrix becomes

$$\begin{pmatrix} a_{N+1} \\ b_{N+1} \end{pmatrix} = (\mathbf{PQ})^N \mathbf{P} \begin{pmatrix} a_0 \\ b_0 \end{pmatrix}. \quad (7)$$

In the CROW-MZI shown in Fig. 2, a dividing Y-branch evenly distributes the optical field between the ridge waveguide and CROW sections of the interferometer, while an adding Y-branch combines the fields that have traveled the separate paths. Thus light is input only at one port of the CROW section and the output field amplitudes for this arm are given by Eq. 6, with \mathbf{T} defined by Eq. 7. At the combining Y-branch the field in the ridge waveguide arm has accumulated an optical phase and loss given by $\exp(-(\alpha + i\beta)L)$ in a length L . The output transmitted power is proportional to the square of the summed complex amplitudes of the fields passing through the two arms

$$output \propto \left| C - \frac{AD}{B} + e^{-(\alpha+i\beta)L} \right|^2. \quad (8)$$

Finally, this simple analysis method does not incorporate waveguide dispersion, typically a linear function of wavelength, nor does it account for the wavelength dependence of the coupling coefficient, which can vary significantly over the large bandwidth measured here.

In Fig. 5 we show the theoretical fit (blue) of the CROW-MZI transmission, superimposed on the experimental data (black). A wavelength range of approximately 30 nm is shown to more clearly show the detail of the fit to the data. The parameters used for the fit are noted in the caption of Fig. 5 and are consistent with expected values. Using these parameters, the intrinsic CROW response is given by Eq. 6. The qualitative agreement in Fig. 5 between the theory and experiment is remarkable considering the many simplifying assumptions described above. Clearly the precision of the fabrication was sufficient to validate our assumptions and confirm the theory.

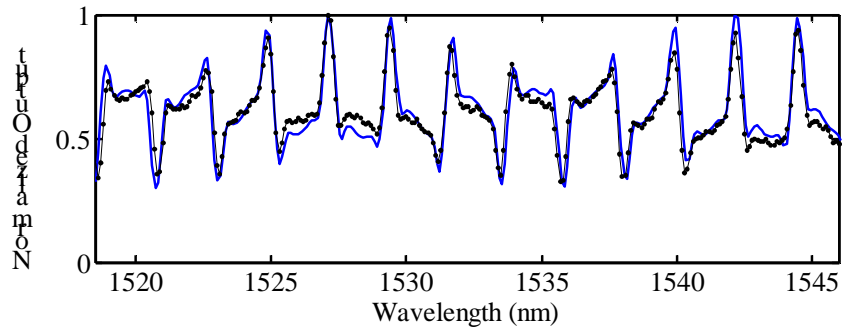


Fig. 5. Experimental data (black) and the theoretical fit (blue) based on Eq. 8. The fitting parameters used for the fit were: polarization 93% TE and 7% TM, effective indices 1.48475 for TE and 1.48555 for TM, power coupling coefficients 0.46 for TE and 0.85 for TM, and waveguide loss of 30 dB/cm.

4. Conclusion

We have demonstrated at telecommunications wavelengths a novel polymeric MZI geometry that uses serially coupled microresonators. In a conventional MZI, light that traverses two separate optical paths interferes after accumulating different optical phases. The optical paths typically differ only in the effective optical length so that only a phase difference, but no intrinsic amplitude response, is incurred in each arm. Here, however, one path is a ridge waveguide, while the other arm consists of coupled resonators. The response of the coupled resonator arm exhibits not only more complicated phase properties (similar to those calculated in [6-8]) than a simple ridge waveguide, but also a periodic spectral response of the absolute field amplitude. Thus the overall transmission is a mixture of the interference of different phases accumulated in the two arms of the device, and the spectral amplitude response of the CROW arm. Although these phenomena cannot be simply decoupled in a CROW with a finite number of resonators, the simple matrix model used to analyze the CROW-MZI shows good agreement with the measured spectral output. The agreement of the experimental data and the theoretical fit, using the assumption of exactly equal ring radii and coupling coefficients, attests to the precision of the fabrication.

Acknowledgments

This work was supported in part by the Office of Naval Research, the Defense Advanced Research Project Agency, and the National Science Foundation. The authors are pleased to acknowledge the helpful discussions with Joyce Poon, and Dr. Jacob Scheuer.